Chemosphere 238 (2020) 124560

Contents lists available at ScienceDirect

Chemosphere

journal homepage: www.elsevier.com/locate/chemosphere

Physical interactions between marine phytoplankton and PET plastics in seawater

Silvia Casabianca [a, b, **], Samuela Capellacci [a, b], Antonella Penna [a, b], Michela Cangiotti [c], Alberto Fattori [c], Ilaria Corsi [d], Maria Francesca Ottaviani [c], Riccardo Carloni [c, *]

[a] Department of Biomolecular Sciences, Campus E. Mattei, Via Cà le Suore 2/4, 61029, Urbino, PU, Italy
[b] Conisma, Consorzio di Scienze Interuniversitario sul Mare, Piazzale Flaminio 6, 00136, Rome, Italy
[c] Department of Pure and Applied Sciences, Campus E. Mattei, Via Cà le Suore 2/4, 61029, Urbino, PU, Italy
[d] Department of Physical, Earth and Environmental Sciences, University of Siena, Italy

HIGHLIGHTS

- Adhesion rate of phytoplankton on plastics in artificial seawater was studied.
- Interaction mechanism of phytoplankton with plastics was investigated by EPR.
- Diatom shows an exponentially-increasing adsorption on plastic surface over time.
- Dinoflagellate has a reduced interaction strength and rolls on the plastic surface.
- Siloxane groups of diatom frustule bind to the hydrophobic plastic surface.

GRAPHICAL ABSTRACT

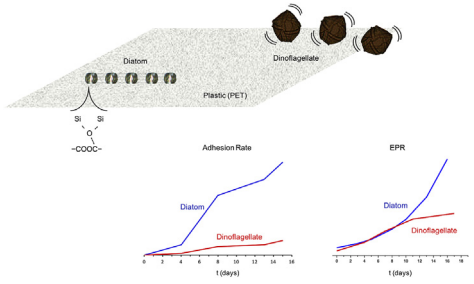

ARTICLE INFO

Article history:
Received 17 May 2019
Received in revised form
24 July 2019
Accepted 9 August 2019
Available online 10 August 2019

Handling Editor: Tamara S. Galloway

Keywords:
Adhesion rate
Electron paramagnetic resonance
Lingulodinium polyedrum phytoplankton
Skeletonema marinoi

ABSTRACT

Plastics are the most abundant marine debris globally dispersed in the oceans and its production is rising with documented negative impacts in marine ecosystems. However, the chemical-physical and biological interactions occurring between plastic and planktonic communities of different types of microorganisms are poorly understood. In these respects, it is of paramount importance to understand, on a molecular level on the surface, what happens to plastic fragments when dispersed in the ocean and directly interacting with phytoplankton assemblages. This study presents a computer-aided analysis of electron paramagnetic resonance (EPR) spectra of selected spin probes able to enter the phyoplanktonic cell interface and interact with the plastic surface. Two different marine phytoplankton species were analyzed, such as the diatom *Skeletonema marinoi* and dinoflagellate *Lingulodinium polyedrum*, in absence and presence of polyethylene terephthalate (PET) fragments in synthetic seawater (ASPM), in order to *in-situ* characterize the interactions occurring between the microalgal cells and plastic surfaces. The analysis was performed at increasing incubation times. The cellular growth and adhesion rates of microalgae in batch culture medium and on the plastic fragments were also evaluated. The data agreed with the EPR results, which showed a significant difference in terms of surface properties between the diatom and dinoflagellate species. Low-polar interactions of lipid aggregates with the plastic surface sites were

* Corresponding author.
** Corresponding author. Department of Biomolecular Sciences, Campus E. Mattei, Via Cà le Suore 2/4, 61029, Urbino, PU, Italy.
E-mail addresses: silvia.casabianca@uniurb.it (S. Casabianca), r.carloni1@campus.uniurb.it (R. Carloni).

https://doi.org/10.1016/j.chemosphere.2019.124560

mainly responsible for the cell-plastic adhesion by *S. marinoi*, which is exponentially growing on the plastic surface over the incubation time.

1. Introduction

Every year, millions of tons of plastic material flow into the oceans. Over the past few months, there has been an increasing public and political concern about marine pollution, not only for the highly negative impact on the marine organisms, but also for the cascade onto environmental issues related to climate changes (Derraik, 2002; Obbard et al., 2014; Windsor et al., 2019; Fang et al., 2017; Horton and Dixon, 2017). The ubiquitous nature of plastics and microplastics led to their accumulation along the water column and on the bottom of the oceans over the last decades. It is generally assumed that much of this plastic debris persists on the ocean surface for years or even decades (Van Sebille et al., 2012; Cozar et al., 2014) due to the robustness of plastics and the fact that more than 50% of polymers have a density lower than that of seawater (Andrady, 2011), allowing durable and persistent substratum for the bio-adhesion of marine organisms. In fact, plastics can represent the carrying way of many organisms, including not allochthonous species, to new habitats altering the endemic communities. Floating plastics can transport disease vectors through the sea or absorb biotoxins, chemical, and organic pollutants. (Zettler et al., 2013; Reisser et al., 2014; Fazey and Ryan, 2016; Casabianca et al., 2019). But it is also known that plastics are subjected to sinking especially due to the microorganism colonization which favors the formation of hetero-aggregates or general aggregates (Long et al., 2015; Moriceau et al., 2017). The biofouling or bio-adhesion can modify the density of particles and buoyant particles may, in the end, sink to the bottom. Microalgal and microbial adhesion, and subsequent colonization on plastic fragments occur quickly (Bakker et al., 2003; Zettler et al., 2013; Oberbeckmann et al., 2015). The sticking ability is mediated by the phytoplankton polysaccharide excretion that may coagulate due to turbulence to form sticky particles or TEPs (transparent exopolymer particles) allowing the microalgal cell aggregation to TEP (Passow, 2002; Bhattacharya et al., 2010). These aggregates transport the phytoplanktonic cell and marine detritus to the sea bottom along the water column. Microplastics can be incorporated in these aggregates and transported as well to the sea floor (Long et al., 2015). Furthermore, the marine aggregates incorporating microplastics are food for grazers, gaining access to the higher levels of the trophic web (Carson, 2013; Farrell and Nelson, 2013). Therefore, both sinking and ingestion of microplastics through adhesion/aggregation to microbiota have a significant impact on marine ecosystems (Cole et al., 2013; Kiessling et al., 2015). It is also known that the biological adhesion to plastics is mediated by the hydrophobic surface that seems to stimulate the colonization of microorganisms by biofilm formation and the rapid succession of microbial communities (Zettler et al., 2013).

In this study, the computer-aided analysis of electron paramagnetic resonance (EPR) spectra was carried out as a first attempt to provide a suitable method for investigating the interactions occurring between the microalgal cells and plastic surfaces. Marine diatom *Skeletonema marinoi* and *Lingulodinium polyedrum* have been grown in the presence and absence of polyethylene terephthalate (PET) fragments in synthetic seawater to *in-situ* characterize the interactions occurring between the microalgal cells and plastic surfaces. For this purpose, a selected spin probe was added in solution. Previous studies of similar systems have already demonstrated the ability of the spin-probe EPR technique to obtain *in-situ* structural and dynamical information on interactions occurring in the medium (Casabianca et al., 2018; Deriu et al., 2017; Nguyen et al., 2017; Andreozzi et al., 2017; Ottaviani et al., 2014; Ottaviani et al., 2012; Mishraki et al., 2011). After an accurate screening, we selected the surfactant spin probe 4-dodecyldimethylammonium-2,2,6,6-tetramethyl-piperidine-N-oxide bromide (CAT12), which has a double advantage: (a) to monitor the cell-plastic interactions; its surfactant nature favors the insertion into the cell membrane, but also well adapt at the hydrophobic plastic surface in contact with salted water, due to the presence of both an hydrophobic chain and a charged polar head; (b) as a surfactant, CAT12 works as a water pollutant and it becomes an important ingredient of the system, also reporting about the interacting properties of surfactants and lipids with plastic and algal cells in the seawater. With the aim to investigate interactions on a time-scale basis, the analysis was performed at increasing incubation times, up to 16 days. We will discuss separately, in a comparative way, the results obtained from the two different phytoplanktonic species.

2. Materials and methods

2.1. Microalgal culture conditions

The diatom *Skeletonema marinoi* CBA4 and dinoflagellate *Lingulodinium polyedrum* VGO1024 were maintained in F/2 and L/1 medium (Guillard, 1975) respectively. Culture conditions were 16 ± 1 °C and 23 ± 1 °C for the diatom and dinoflagellate species, respectively, under a standard 12:12 h light-dark cycle. Light was provided by cool-white fluorescent bulbs (photon flux of 100 $\mu E\, m^{-2} s^{-1}$).

2.2. Adhesion rate of microalgal species to the plastic substrate

All experiments were performed in sterile polycarbonate flasks. The artificial seawater ASPM (Artificial Seawater Provasoli-McLachlan) base (Guillard, 1975), enriched with F/2 and L/1 medium components, was used as medium in each condition to have comparable results, not affected by natural seawater usually used in media preparation. *S. marinoi* CBA4 (initial concentration of 1.0×10^5 cells/mL) and *L. polyedrum* VGO1024 (initial concentration of 1.0×10^4 cells/mL) were grown in 50 mL flasks containing 40 mL of sterilized medium together with PET (polyethylene terephthalate) sheets (4 mm × 20 mm) obtained from sterilized PET bottles. Similar PET fragments can be found in seawater as a product of degradation of water bottles. Culture conditions were those described above. A single plastic sheet was harvested every four days since the inoculum, and gently scraped in 2 mL of sterile seawater. Cell amount was evaluated using Sedwhich-Rafter chamber under an inverted microscope (ZEISS Axiovert 40CFL) at 400X magnification. Cell abundance was expressed as cells/mL for cultures and cells/mm^2 for cells attached to the plastic surface. The growth and the adhesion rates, defined respectively as the rate of increased abundance in culture and on the plastic sheets, were calculated on the basis of the longest possible period of exponential

growth using the equation: $\mu = \ln (Nt/N0)/\Delta t$, where N is the number of cells/mL (for growth rate) or the number of the plastic adherent cells expressed as cells/mm^2 (for adhesion rate) and Δt the time interval expressed in days.

2.3. EPR analysis

2.3.1. Samples preparation

Together with light microscopy counting, EPR analyses were performed. Experimental conditions were the same described for adhesion rate determination. Samples for EPR analysis were obtained using a final concentration of 1 mM of CAT12 probes in ASPM medium. This solution (2 mL) in absence and in presence of the microalgae (0.45 cells/mL) was analyzed by EPR in absence and presence of the plastic sheet. The solutions were left equilibrating for 2 h before starting the analysis. The plastic sheets after equilibration were gently dried on a filter paper, while the supernatant was collected and inserted into an EPR tube. The EPR spectra were recorded for the solutions and for the plastic strips. The latest were assembled making them adhere on a glass rod using parafilm before the insertion into the EPR cavity.

The following samples were analyzed as control references: (i) the culture media (ASPM F/2 and ASPM L/1), (ii) *S. marinoi* and *L. polyedrum* cell cultures without plastic sheets and (iii) plastic sheets maintained in ASPM F/2 and ASPM L/1 without cultured cells.

2.3.2. Instrumentation

EPR spectra were recorded by means of an EMX-Bruker Spectrometer operating at X band (9.5 GHz) and interfaced with a PC (software from Bruker). The temperature was controlled with a Bruker ST3000 variable-temperature assembly cooled with liquid nitrogen.

2.3.3. EPR spectra computation

Simulation of the EPR line shape was performed by using Budil et al. program (Budil et al., 1996). The main parameters extracted from computation were: (a) the g_{ii} values measuring the coupling between the electron spin and the magnetic field. These values were assumed constant that is $g_{ii} = 2.009, 2.006, 2.003$, on the basis of previous studies on similar systems (Kontogiannopoulos et al., 2018; Deriu et al.). (b) the A_{ii} values measuring the coupling between the electron spin and the nitrogen nuclear spin. We assumed $A_{xx} = A_{yy} = 6$ G in all cases to limit the number of variables as already done in previous studies (Kontogiannopoulos et al., 2018; Deriu et al.). Therefore, only A_{zz} was changed. When the spectrum lines are narrow (Free component), the error of the A_{zz} parameter is ±0.01 G. This error increases for the spectra constituted by broader lines, up to ±0.1 G; (c) the correlation time for the diffusion rotational motion of the probe, τ, which measures the microviscosity and therefore reports on the interactions occurring between the probe and the environmental molecules or interacting sites (error ± 0.01 ns, one order of magnitude lower for the Free component); and (d) the line width, which measures the spin-spin interactions between probes in close positions, measuring the proximity of interacting sites (error ± 0.1 G).

The total intensities, calculated by double integration of the overall EPR spectra, provide a measure of the concentration of paramagnetic species in the samples. Finally, since two signal components, due to probes sitting in two different environments, constitute the spectra, the subtraction of spectra from one another allowed us to extract each signal and then compute it. The double integration of each signal referred to the double integral of the spectra gives the relative percentage of the probes in each environmental condition (error ± 0.5%).

2.4. Statistical analyses

Data analyses were performed using nonparametric Mann-Whitney and Spearman correlation tests using PAST ver. 2.17 (Hammer et al., 2001) with a p-value < 0.05 determining significance.

3. Results and discussion

3.1. Growth and adhesion rate on the plastic surface of microalgal species

In the same batch culture, during the exponential growth phase, a significant positive correlation (Spearman's rs = 0.61, p = 0.01) between *S. marinoi* free-living abundance and *S. marinoi* abundance attached to plastic sheets was found. Thus, a higher abundance in the culture was directly linked to an increased abundance of cells attached to plastics. In particular, the maximum free-living cell amount of *S. marinoi* was $1.6 \times 10^6 \pm 1.6 \times 10^5$ cells/mL, while cell abundance attached to plastics was $3.4 \times 10^5 \pm 8.5 \times 10^4$ (corresponding to $8.5 \times 10^3 \pm 2.1 \times 10^3$ cells/mm^2). The adhesion rate of *S. marinoi* cells attached to the plastics was calculated during the exponential growth phase with a value of 0.15 d^{-1}.

No correlation between *L. polyedrum* abundance in culture and *L. polyedrum* attached to plastic sheets was found (Spearman's rs = 0.31, p = 0.32). During the growth phase, *L. polyedrum* reached the abundance of $2.1 \times 10^4 \pm 5.9 \times 10^3$ cells/mL^1 while cell abundance attached to plastics was 62 ± 22 (corresponding to 2 ± 1 cells/mm^2). The adhesion rate of *L. polyedrum* cells attached to plastic was 0.06 d^{-1}. The growth curves of cells attached to the plastic surface of the two-species showed that *L. polyedrum* retained much lower abundance to the plastic sheets of two orders of magnitude smaller than *S. marinoi* (Fig. 1).

3.2. EPR study

3.2.1. Diatom Skeletonema marinoi interactions with plastic surface

Fig. 2A shows an example of an experimental EPR spectrum obtained from a plastic fragment extracted after 16-days incubation in the *S. marinoi* batch grown in ASPM medium enriched with nutrients and CAT12.

As indicated in Fig. 2A with arrows, two components constitute the spectra: (a) a three-narrow lines component, which is characteristic of free-moving CAT12 probes. However, as we will describe

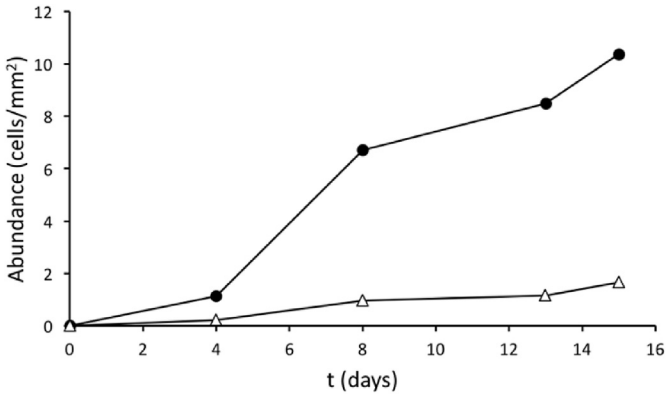

Fig. 1. Amount adhesion of marine diatom *Skeletonema marinoi* CBA4 (●) and dinoflagellate *Lingulodinium polyedrum* VGO1024 (Δ) to plastic sheets in cultured conditions over the studied period. Abundance is reported as *S. marinoi* (x 10^3) and *L. polyedrum* (x 10^0) cells/mm^2.

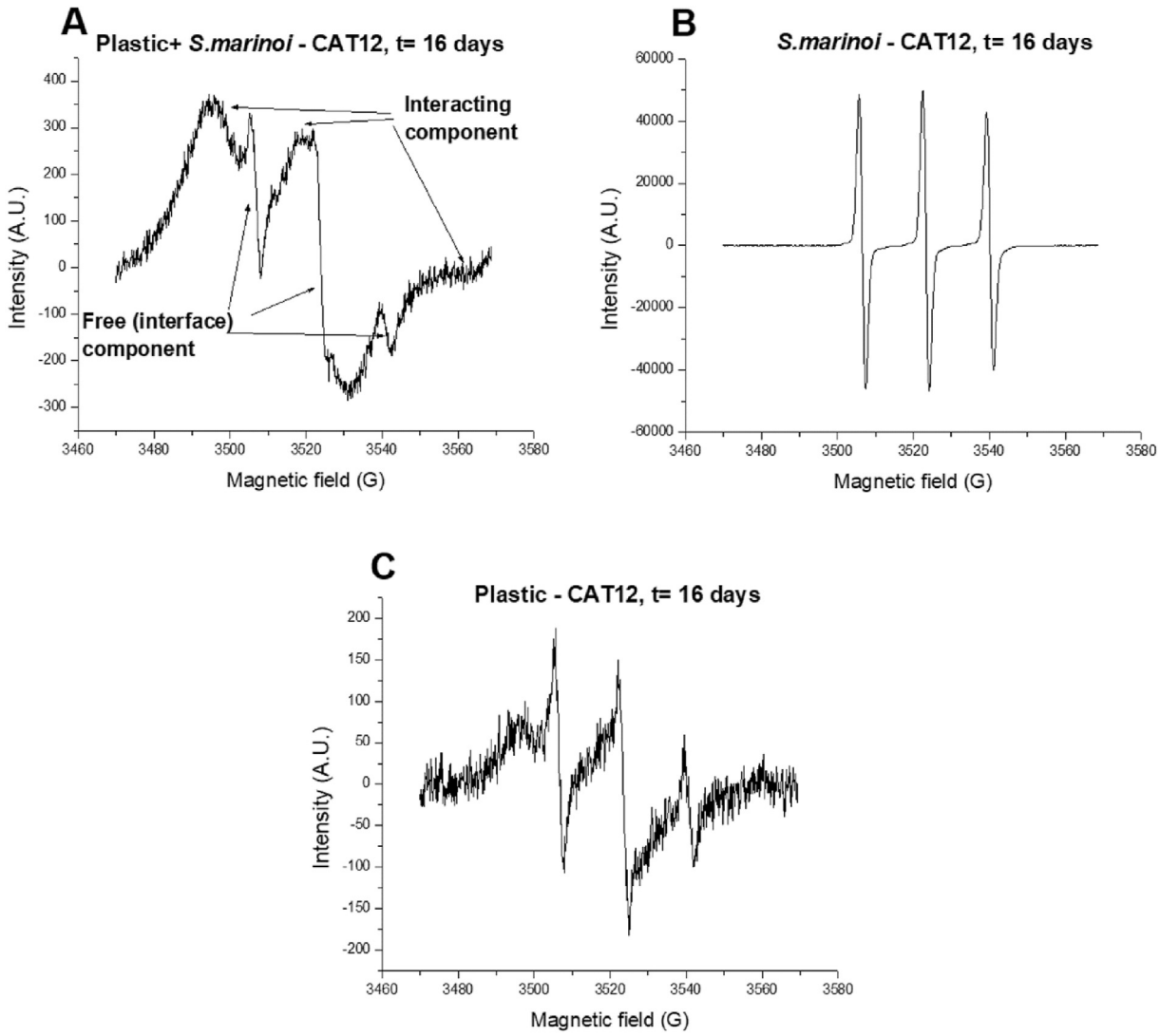

Fig. 2. Experimental EPR spectra obtained from: A) a plastic fragment (simply termed "plastic") extracted after 16-days incubation in the *S. marinoi* batch grown in ASPM medium enriched with nutrients and CAT12; B) CAT12 in the *S. marinoi* batch culture; C) plastic extracted from the medium in the absence of *S. marinoi* after 16 days of incubation.

hereafter, the mobility of these probes was significantly lower than those in the medium incubated with *S. marinoi*, indicating that these "free" probes were located at the polar (solvent) interphase; (b) an anisotropic signal (the lines split into X, Y, and Z components) with broader lines. The anisotropy arises from the slowing down of the probe rotational motion after interaction with environmental molecules or interacting sites, like those at the plastic and/or the cell surface. For this reason, this component was called "interacting" component.

The spectrum of CAT12 in the *S. marinoi* batch culture, shown in Fig. 2B, was only constituted by the Free component and differed from the spectra obtained in the supernatant solutions after adsorption in the intensities (in arbitrary units = A.U.) and in the rotational motion, as described hereinafter. Conversely, as shown in Fig. 2C, the spectrum of the plastic extracted from the medium in the absence of *S. marinoi* after 16 days of incubation also shows the two components as in the presence of the algal cells, but we visually note that there are significant differences, like: i) the intensity, higher in presence than in absence of *S. marinoi*; ii) the relative amounts of the two spectral components, being the interacting one in higher relative amount in presence of *S. marinoi*; and iii) the line shape of the interacting component, being the lines more resolved in presence than in absence of the *S. marinoi*.

First, by double integration of the spectra, the total intensities were calculated. The variations in absolute intensities as a function of the equilibration time for all the liquid media - the supernatants with and without the cells after adsorption on plastic, and the *S. marinoi* culture in the absence of plastics - are reported in Fig. 3A in the form of percentages, referring to the spectrum with the maximum intensity as a 100% intensity.

First, we note that the adsorption of CAT12 on plastic is already happening since $t = 0$, enhanced in the presence of *S. marinoi*. Indeed, *S. marinoi* increased the solubility of CAT12 due to the insertion of the C12 chain into the cell membrane. When *S. marinoi* cells are present, the intensity in the supernatant solutions significantly decreased over time due to the adhesion of the cells to the plastic surface.

In any case, also in the *S. marinoi* medium in absence of plastic, the intensity decreased over time. This mainly happened in the first 3 days and then, from 3 to 8 days, the intensity poorly changed. After 8 days the decrease was very slow. We may ascribe this effect to the presence of antioxidants into the cells (Andreozzi et al.,

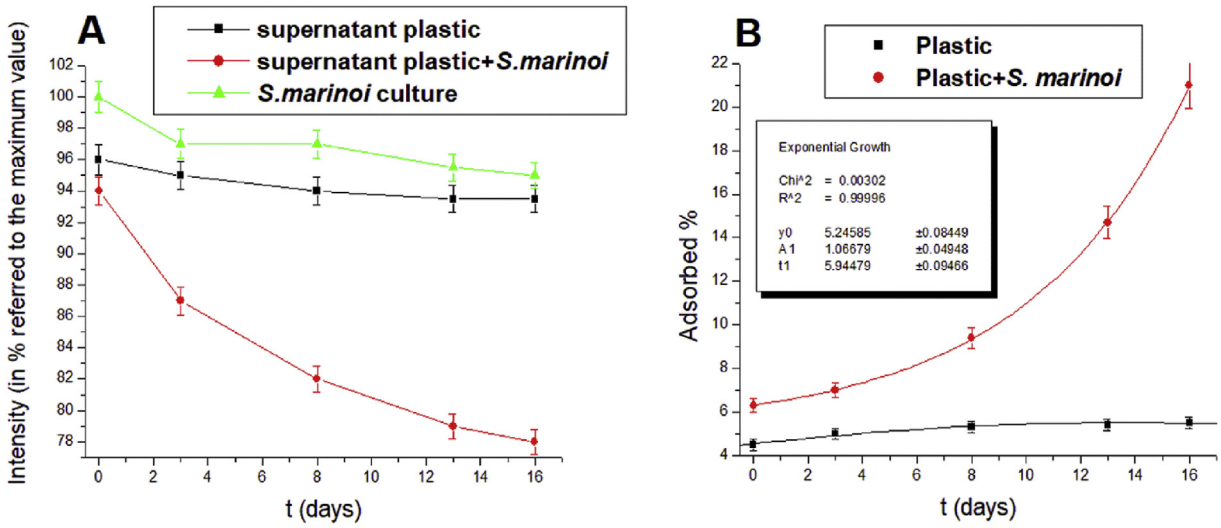

Fig. 3. A) Variations in absolute intensities of the EPR spectra as a function of the equilibration time for all the liquid media: the supernatants with and without the cells after adsorption on plastic, and the *S. marinoi* culture in the absence of plastics Intensity values are reported in form of percentages, referring to the spectrum with the maximum intensity as a 100% in intensity; B) adsorption percentages of CAT12 onto the plastic, in the absence and presence of *S. marinoi*, as a function of the incubation time. The variation in the presence of *S. marinoi* was fitted as exponential growth.

2017). In the absence of plastics, the probe was free to partially cross the cell membrane and got slightly exposed to the antioxidants in the cytosol.

The intensity ratios between the solutions before adsorption and the supernatants after adsorption allowed us to obtain the adsorption percentages of CAT12 onto the plastic, in the absence and presence of *S. marinoi*, as a function of the incubation time, shown in Fig. 3B.

Interestingly, the adsorbed percentage in the presence of *S. marinoi* increased over time, perfectly fitting an exponential growth, demonstrating the good choice of the probe, able to follow the fate of *S. marinoi* cells in the adhesion process with the plastic. In the absence of *S. marinoi*, the adsorbed percentage was low and poorly changed over time. The increase in the adsorbed percentage obtained from the supernatant medium strictly resembles the increase in the absolute intensity of the spectra of the plastic.

The two spectral components obtained from the plastic samples were extracted from each other by using a subtraction procedure, that is, subtracting one from another spectrum recorded for the same sample in slightly different experimental conditions, thus containing the two identical components but in different relative amounts. This procedure allowed us to evaluate the relative percentages of the two components by double integration of each of them. Fig. 4 shows the variation of the relative percentage of Interacting component for the plastic in the absence and presence of *S. marinoi* as a function of the equilibration time.

In the absence of *S. marinoi*, the relative amount of Interacting component was about 43% and almost did not change over time. Conversely, in the presence of *S. marinoi*, the relative amount of interacting probes was about 68% at $t = 0$, and a progressive increase occurred during the 17 days of incubation. This means that the increased adsorption evidenced in Fig. 3 from the absence to the presence of *S. marinoi* and increasing over time is now confirmed as due to increased availability of interacting sites created by *S. marinoi*, which promotes its adhesion to the plastic. We know that *S. marinoi* cells are characterized by an amorphous silica coating and a parallelepiped shape connected to form strings. Both the shape and the amorphous silica coating may be considered as responsible for the cell adhesion to the hydrophobic plastic. Indeed, amorphous silica contains both polar and low polar sites, namely the SiOH and Si-O-Si groups. Mainly the latter sites may interact with the hydrophobic plastic surface. However, PET also contains −COO- groups which may generate dipole-dipole interactions with the SiOH groups of the silica surface.

Further precious information came from a deep analysis of the spectral line shape. The above-described subtraction procedure led to extract the Free and the Interacting components from each spectrum of plastic samples. As described in the experimental section, these components were computed by using the well-established computation procedure of Budil et al., (1996)

Fig. 4 shows some selected examples of computations of the Free and Interacting components. The main parameters used for computation (A_{ii}, τ, and line width) are listed in the legends. The spectra are normalized in heights (intensity in the y-axis = 1). Other examples of computation are shown in the Supplementary Information (Figs. S1 and SI).

As a matter of comparison, Fig. 4 shows the computations of both the spectrum of the supernatant solutions and the Free component of the plastic samples, which did not change over time. The two computations provided very different values of A_{zz} (the micropolarity parameter) and τ (the microviscosity parameter, measuring the interaction strength). The Free component at the plastic interface shows higher micropolarity and microviscosity with respect to that of the probes which remain free in the medium. This means that the salted medium concentrated in small drops at the plastic surface. The reproducibility of this effect, also over time, confirms this interpretation.

However, in the presence of *S. marinoi*, the microviscosity parameter of the Free component showed to change over time, even if the micropolarity remained almost unaffected. Fig. 5 shows the variation of τ as a function of the equilibration time for the Free (interface) component in the absence and presence of *S. marinoi*.

Interestingly, in this case too, the variation of the parameter is well fitted by using an exponential growth model. This means that *S. marinoi* cells, interacting in increasing amounts at the plastic surface over time, are progressively compressing the medium drops at the cell/plastic interface.

Going back to Fig. 4, the computations of the interacting components also show interesting trends. First, the micropolarity parameter, A_{zz}, significantly decreases for the CAT12 probes from

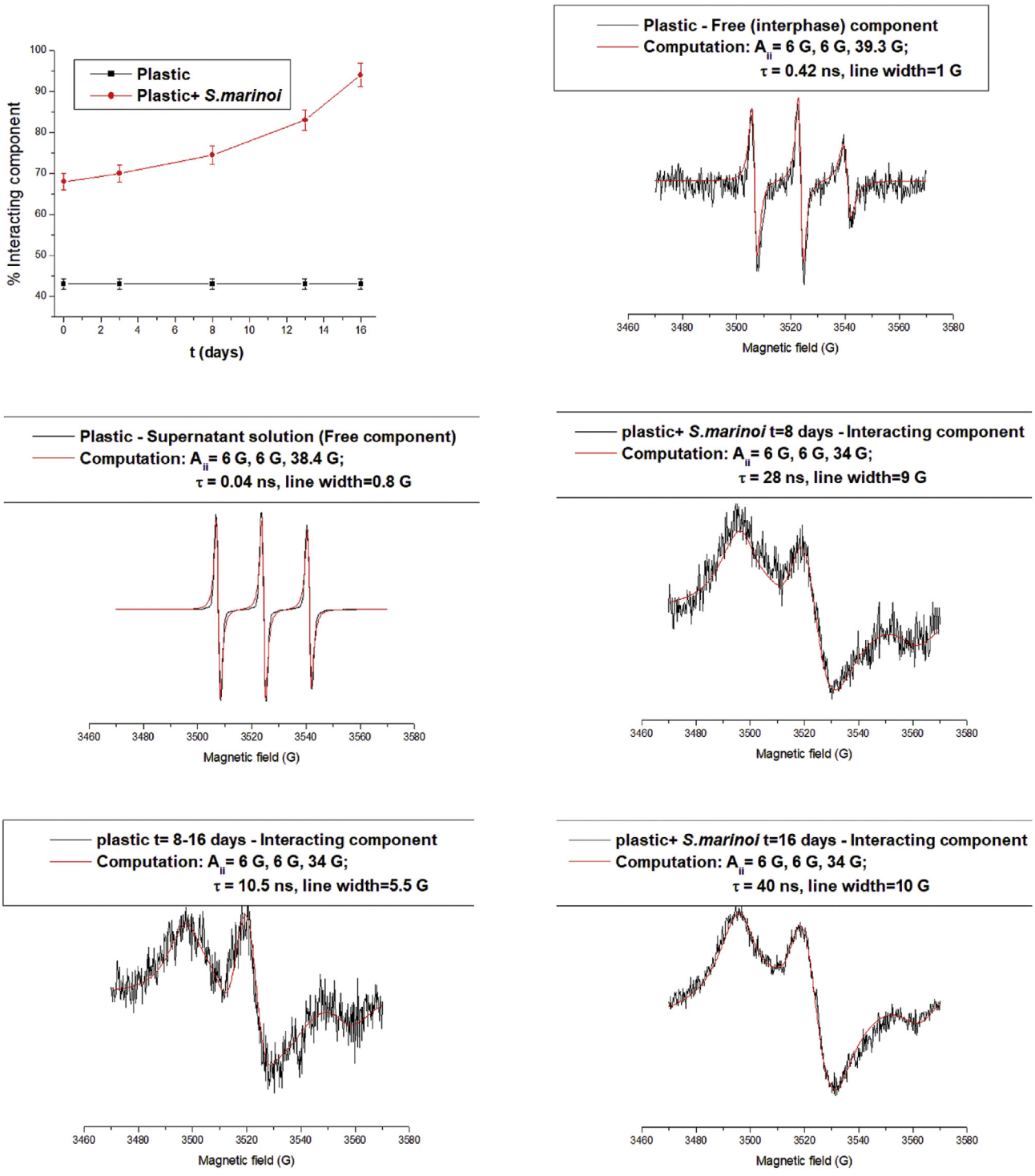

Fig. 4. Variation of the relative percentage of Interacting component in the absence and presence of *S. marinoi* as a function of the equilibration time and selected examples of experimental (black lines) and computed (red lines) Free and Interacting components. The main parameters used for computation (A_{ii}, τ, and line width) are listed in the legends. The spectra are normalized in heights (intensity in the y-axis = 1). (For interpretation of the references to colour in this figure legend, the reader is referred to the Web version of this article.)

the solution (38.4 G) to the plastic-interacting conditions (34 G). This means that these probes are approaching the hydrophobic plastic surface, in spite of the charged heads containing the nitroxide radical groups, promoted by the presence of the hydrophobic C12 chain. Therefore, surfactants and lipids like CAT12 well interact with the plastic surface in the seawater. The occurrence of strong interaction is proved by the high value of the microviscosity parameter, τ. This strong interaction cannot match with a weak hydrophobic interaction, but the increase in line width provides another piece of information: the occurrence of cooperative interaction, that is, the formation of CAT12 aggregates at the plastic surface. So, the surfactants and lipids well interact with the plastic

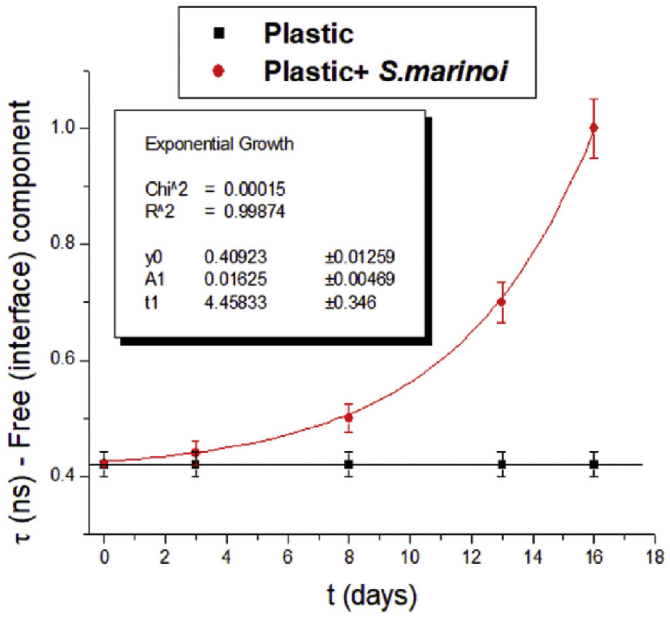

Fig. 5. Variation of the microviscosity parameter, τ, as a function of the equilibration time for the Free (interface) component of plastic samples in the absence and presence of *S. marinoi*.

surface by forming aggregates. However, the situation is different in the absence and presence of the *S. marinoi*, as better demonstrated by analyzing Fig. 6, which shows the variations of the microviscosity parameter, τ (Fig. 6A), and the line width (Fig. 6B) as a function of the equilibration time for the Interacting component in the absence and presence of *S. marinoi*.

Again, the increase of the microviscosity parameter as a function of the incubation time in the presence of *S. marinoi* is fitted by an exponential growth model, indicating that *S. marinoi* cells are exponentially increasing their adhesion to the plastic, by means of low-polar interactions of the lipid aggregates, arising from the cell membrane. The line width also increases, even if this increase does not follow an exponential pattern, but an almost linear increase from 0 to 13 days and then it remains nearly unchanged from 13 to 17 days. However, we must take into consideration that this increase is lower than expected since it probably compensates the decrease in line width found between 0 and 8 days in the absence of *S. marinoi*. This decrease indicates that the CAT12 surfactants redistributed at the plastic surface in the 0–8 days range of time. Conversely, in the presence of *S. marinoi*, CAT12 surfactants cooperated with *S. marinoi* cell membrane lipids to form more packed aggregates, progressively (exponentially) crammed on the plastic surface over time. The exponential growth tested by EPR for *S. marinoi* at the plastic surface is in good agreement with the results described in Fig. 1.

3.2.2. *Dinoflagellate Lingulodinium polyedrum interactions with plastic surface*

L. polyedrum cultured samples show different results with respect to *S. marinoi*. However, the EPR spectra and components of *L. polyedrum samples* and their computations look similar to those shown for *S. marinoi* in Figs. 2 and 4 and Fig. S1 in the SI. Some examples of the interacting components and their computations for *L. polyedrum* samples are shown in the Supplementary Information (Fig. S1). Fig. 7 reports the variations over the equilibration time of the following parameters: the adsorbed percentage (A); the intensities (in form of percentage) of the supernatant of plastic, in the absence and presence of *L. polyedrum*, and for the *L. polyedrum* culture (B); the relative percentage of interacting component (C); the correlation time for the rotational diffusion motion of the probe, τ, for the interacting (D) and the free (E) components, measuring the microviscosity, and, in turn, the strengths of interaction.

For a better comparison with the results from *S. marinoi* samples, the same parameters variation range is considered in the Y-axis for the two cells samples.

It is interesting to note that all the parameters are lower and/or undergo to a lower increase over time for *L. polyedrum* if compared to *S. marinoi* in the presence of plastic, in agreement with lower adsorption and interaction with the plastic surface for the former with respect to the latter cell culture. This is also in agreement with the adhesion rates shown for the two algae species in Fig. 1. Further information is obtained by analyzing in detail the shape of the parameter variation, as follows:

The variations in the intensity of the EPR spectra of the supernatant solutions over time of *L. polyedrum* (Fig. 7A) and *S. marinoi* (Fig. 3A) in the presence of the plastic are in line with the variations

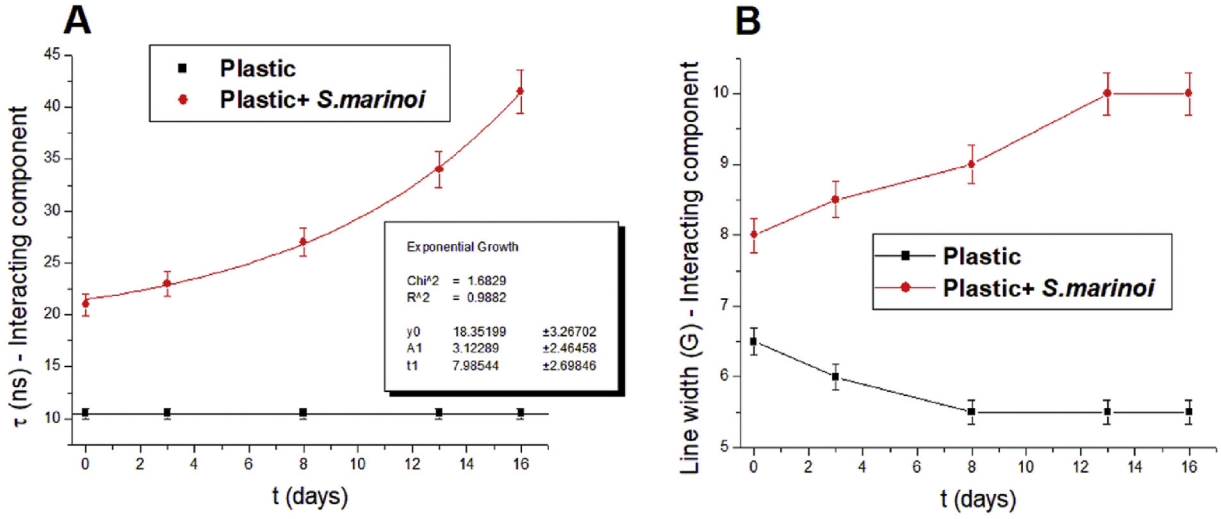

Fig. 6. Variation of the microviscosity parameter, τ (A), and the line width (B) obtained from EPR spectra computations as a function of the equilibration time for the Interacting component in the absence and presence of *S. marinoi*.

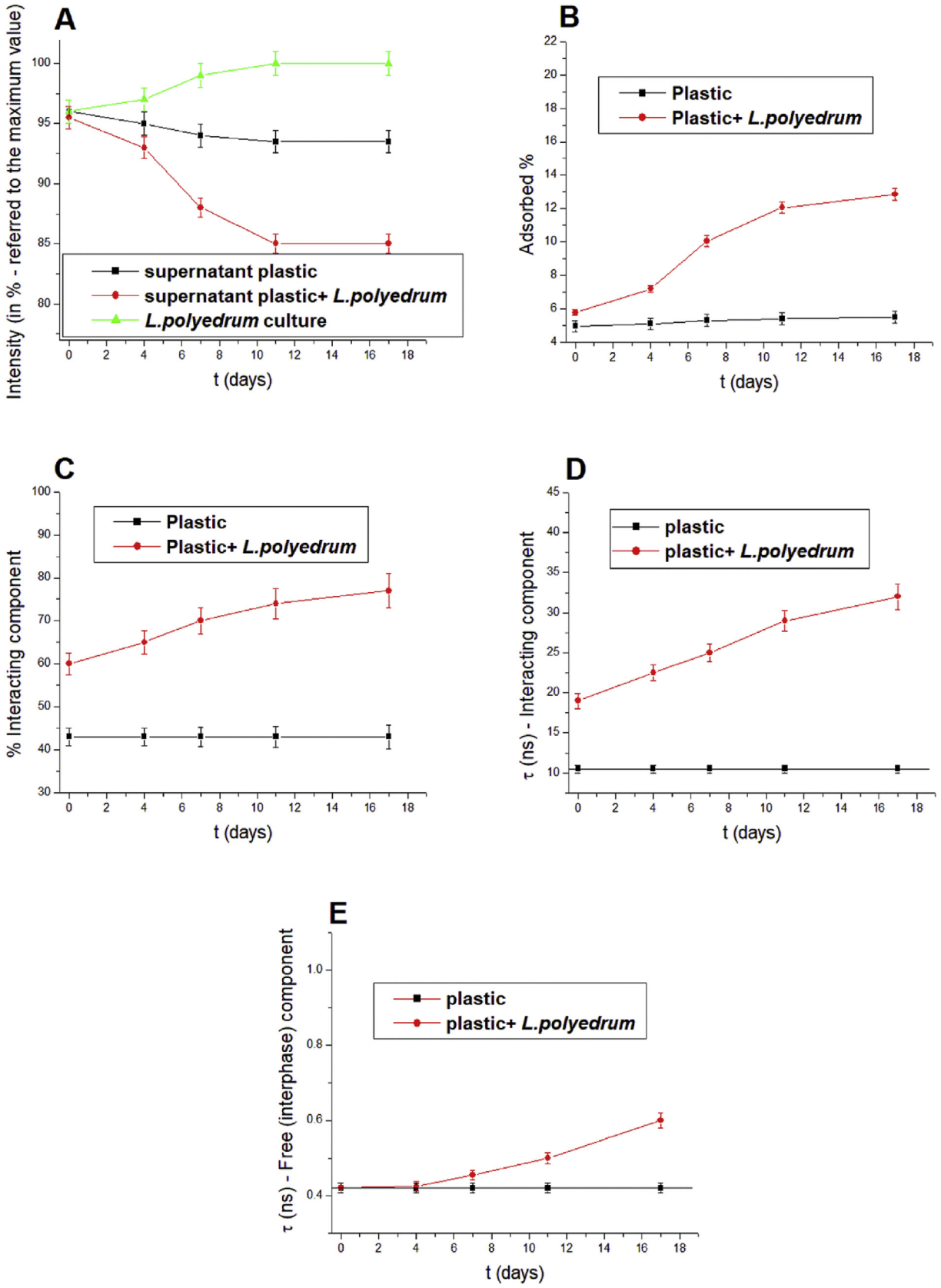

Fig. 7. Variations over the incubation time of the following parameters obtained from the analysis of the EPR spectra of *L. polyedrum* samples: the intensities (in form of percentage) of the supernatant of plastic, in the absence and presence of *L. polyedrum*, and for the *L. polyedrum* culture (A); the adsorbed percentage (B); the relative percentage of interacting component (C); the correlation time for the rotational diffusion motion of the probe, τ, for the interacting (D) and the free (E) components, measuring the microviscosity, and, in turn, the strengths of interaction.

of the adsorbed percentage in Figs. 7B and 3B. In the presence of plastic, in the first hours (mainly between 4 and 7 h) the adsorbed amount is higher for *L. polyedrum* (Fig. 7A and B) with respect to *S. marinoi* (Fig. 3A and B). The cellulose external frustule of the large (30 μm) *L. polyedrum* cells well adsorbs the CAT12 probes in the plastic interface when the cells precipitate on the surface. However, the *L. polyedrum* cells poorly adhere to the plastic surface and "roll" on the surface impeding further probe adsorption. Conversely, the silica external frustule of the smaller (10 μm) *S. marinoi* cells interacts with the plastic surface. Therefore, the CAT12 probes adsorbed at the cell surface follow the cell/plastic adhesion process, which is exponentially increasing over time.

It is worth to note the difference in intensity variation between the two cell cultures in the absence of plastic (Fig. 7A versus Fig. 3A). In detail, for *L. polyedrum* the CAT12 intensity increases over time, mainly between 4 and 7 h. This indicates that the cellulose casing of these cells well entraps the CAT12 probes with a kinetics of 7 h, also justifying the increased adsorbed percentage of probes in this time range in Fig. 7B, but it poorly interacts with the plastic surface. Conversely, the decrease in intensity for CAT12 adsorbed by *S. marinoi* cells culture (Fig. 3A) is ascribed to a partial internalization of the probes into the cells, getting in touch with antioxidants in the cytosol. Therefore, the exponential increase of the adsorbed percentage for *S. marinoi* in the presence of the plastic (Fig. 3B) is purely due to the increased adsorption/adhesion of the cells with the plastic surface, related to the interaction of the amorphous-silica cell surface with the plastic surface.

Further information comes from the evaluation of the percentage of the interacting component, shown in Fig. 7C for *L. polyedrum*, to be compared with the graph in Fig. 4 for *S. marinoi*. For this latter cell culture, in the presence of plastic, the percentage of interacting component is already higher at $t = 0$ with respect to *L. polyedrum*. However, the percentage of interacting component for *S. marinoi* slowly increases in the first hours, boosting after 8 h. This boost, as discussed above, is related to the exponentially-increasing adhesion of *S. marinoi* onto the plastic. However, unlike *S. marinoi*, *L. polyedrum* shows an increase in the percentage of the interacting component since the first hours while the increase is very poor in the latest hours. This different behavior may be nicely related to different interactions of the two different cell cultures with the probe and the plastic surface, as already discussed for the intensity and adsorbed percentage variations (Figs. 3A-B and 7A-B). The probes adsorbed on the *S. marinoi* silica surface partially enter the cells and "disappear" in the cytosol, from the EPR point of view, due to the antioxidants. The remaining probes are able to monitor the cell adhesion on the plastic surface by means of low-polar interactions of lipid aggregates. Conversely, the probes are adsorbed at the external *L. polyedrum* surface when the cells precipitate on the plastic surface in the drying process, but then the cells roll on the plastic surface without adhering to it, and the percentage of interacting probes cannot increase anymore.

The process of rolling on the plastic surface modifies the interacting strength of the probe at the *L. polyedrum* cell interface, which increases over time (Fig. 7D). Here we have to remember that the interacting probes are those already inserted into the cell membrane, since the C12 chain of the probes enter the lipidic area of the membrane, while the CAT group is embedded in the phospholipid heads layer. However, this interacting-probes fraction is almost absent for the cell cultures in the absence of the plastic, because the CAT group containing the nitroxide radical is free to move at the cell surface. Only plastic adhesion creates this interacting fraction, and, therefore, it reports about the interacting mode and strength. We see that, for both *S. marinoi* and *L. polyedrum*, the probes are compressed in the cell/plastic interface thus increasing the percentage of the interacting component. We suppose that the cell/plastic interaction forces the probes to deeper enter the cell membrane interface decreasing their mobility. For *S. marinoi* the exponential increase accounts for the progressive increase in the strength of interaction because the probes are able to penetrate in the cell interface and measure the adhesion strength of the cells that grow on the plastic. For L. *polyedrum* the interaction strength is much lower, mainly at the earlier times, due to the poor adhesion of these cells with the plastic.

Final confirmation of the different interacting behavior of the two cells cultures with the plastic is obtained by comparing the interacting strength parameter, τ, for the free (interface) component, in Fig. 5 for *S. marinoi* and in Fig. 7E for *L. polyedrum*: the latter only reach 0.6 ns after 17 h (Fig. 7E), while *S. marinoi* shows a value of 1 ns at 17 h of incubation. The weakly interacting probes better report about the cell-plastic interactions than the strongly interacting probes, being well exposed at the external surface of the cells and directly feeling the plastic adhesion. The plastic adhesion is therefore quite poor for *L. polyedrum* if compared to *S. marinoi*.

The line width variation is not reported in Fig. 7 for *L. polyedrum*, because its variation is almost absent over time. Conversely, the increase of line width over time is quite significant for *S. marinoi* (Fig. 6B). The line broadening indicates that, in the *S. marinoi* case, the binding occurs at sites quite close to each other. This accounts for the interaction of lipid aggregates at the *S. marinoi*/plastic interface, while the lipids are poorly aggregated when *L. polyedrum* precipitates on the plastic surface and then rolls over the surface.

4. Conclusions

The analysis of the EPR spectra of CAT12 probes adsorbed on the plastic surface in absence and presence of two different species of marine phytoplankton, diatom *S. marinoi* and dinoflagellate *L. polyedrum*, provides useful information about the mechanism of adhesion of the microalgae on the plastic surface floating on seawater. The CAT12 probes, mimicking the cell membrane components, show that packed cell-components aggregates stabilize at the plastic surface in presence of *S. marinoi*, with an exponentially increasing adsorption as a function of the incubation time. Conversely, *L. polyedrum* shows lower adsorption than *S. marinoi*, and a different mechanism of interaction with the plastic surface. Both the amount of probe adsorbed onto the plastic, and their interaction strength increase exponentially in the presence of *S. marinoi*, following its adhesion rate. Also, the drops of seawater, with a concentrated saline content, are compressed on the plastic surface by *S. marinoi* at the cell/plastic interface. After 17 days, an about 4-times lower amount of probe is adsorbed onto the plastic in absence *S. marinoi*, compared to the sample where this microalga is present. Similarly, the interaction strength is also about 4 times lower. Conversely, *L. polyedrum* shows a reduced interaction strength with the plastic surface, mainly at the earlier times. The probes are initially adsorbed by *L. polyedrum* cells when they precipitate on the plastic surface; but, then, we suppose that these cells start rolling on the plastic surface, due to their poor adhesion to the plastic, favored by their almost cellular spherical shape. Therefore, the probe binding to the plastic is largely prevented and only those adsorbed into the porous cellulose casing of *L. polyedrum* cells remain trapped. The silica frustule of *S. marinoi* cells is more permeable to the probes, mimicking the surfactants/lipids behavior, and the probes, which remain at the external cell surface, well monitor the exponential growth of *S. marinoi* cells at the plastic surface. The siloxane groups of the silica frustule are involved in the binding with the hydrophobic plastic surface and the C12 chain of the spin probes.

This study demonstrates that the use of selected paramagnetic probes and an accurate computer-aided analysis of the EPR spectra,

combined with biological tests, help to *in-situ* clarify the interactions occurring between biological structures and pollutants, or, more importantly, the plastic debris, which are more and more invading the oceans.

Acknowledgements

This article is based on work from COST Action CA 17140 “Cancer Nanomedicine from the Bench to the Bedside” supported by COST (European Cooperation in Science and Technology).

Appendix A. Supplementary data

Supplementary data to this article can be found online at https://doi.org/10.1016/j.chemosphere.2019.124560.

References

Andrady, A.L., 2011. Microplastics in the marine environment. Mar. Pollut. Bull. 62, 1596–1605.
Andreozzi, E., Antonelli, A., Cangiotti, M., Canonico, B., Sfara, C., Pianetti, A., Bruscolini, F.A., Sahre, K., Appelhans, D., Papa, S., Ottaviani, M.F., 2017. Interactions of nitroxide-conjugated and non-conjugated glycodendrimers with normal and cancer cells and biocompatibility studies. Bioconjug. Chem. 28, 524–538.
Bakker, D.P., Klijnstra, J.W., Busscher, H.J., Van der Mei, H.C., 2003. The effect of dissolved organic carbon on bacterial adhesion to conditioning films adsorbed on glass from natural seawater collected during different seasons. Biofouling 19, 391.
Bhattacharya, P., Lin, S.J., Turner, J.P., Ke, P.C., 2010. Physical Adsorption of Charged Plastic nanoparticles affects algal photosynthesis. J. Phys. Chem. C 114 (39), 16556–16561.
Budil, D.E., Lee, S., Saxena, S., Freed, J.H., 1996. Nonlinear-least-squares analysis of slow-motion EPR spectra in one and two dimensions using a modified Levenberg-Marquardt algorithm. J. Magn. Reson. Ser. A 120, 155–189.
Carson, H.S., 2013. The incidence of plastic ingestion by fishes: from the prey's perspective. Mar. Pollut. Bull. 74 (1), 170–174.
Casabianca, S., Capellacci, S., Grazia, M., Dell, C., Tartaglione, L., Varriale, F., Penna, A., 2019. Plastic-associated harmful microalgal assemblages in marine. Environ. Pollut. 244, 617–626.
Casabianca, S., Penna, A., Capellacci, S., Cangiotti, M., Ottaviani, M.F., 2018. Silicification process in diatom algae using different silicon chemical sources: colloidal silicic acid interactions at cell surface. Colloids Surfaces B Biointerfaces 161, 620–627.
Cole, M., Lindeque, P., Fileman, E., Halsband, C., Goodhead, R., Moger, J., Galloway, T.S., 2013. Microplastic ingestion by zooplankton. Environ. Sci. Technol. 47 (12), 6646–6655.
Cozar, A., Echevarría, F., Gonzalez-Gordillo, I.J., Irigoien, X., Úbeda, B., Hernandez-Leond, S., Palmae, A.T., Navarrof, S., García-de-Lomas, J., Ruizg, A., Fernandez-de- Puellesh, M.L., Duartei, C.M., 2014. Plastic debris in the open ocean. Proc. Natl. Acad. Sci. U.S.A. 111, 10239–10244.
Deriu, M.A., Cangiotti, M., Grasso, G., Licandro, G., Lavasanifar, A., Tuszynski, J.A., Ottaviani, M.F., Danani, A., 2017. Self-assembled ligands targeting TLR7: a molecular level investigation. Langmuir 33 (50), 14460–14471.
Derraik, J.G.B., 2002. The pollution of the marine environment by plastic debris: a review. Mar. Pollut. Bull. 44, 842–852.
Fang, X., Hou, X., Li, X., Hou, W., Nakaoka, M., Yu, X., 2017. Ecological connectivity between land and sea: a review. Ecol. Res. 33 (1), 51–61.
Farrell, P., Nelson, K., 2013. Trophic level transfer of microplastic: Mytilus edulis (L.) to Carcinus maenas (L.). Environ. Pollut. 177, 1–3.
Fazey, F.M., Ryan, P.G., 2016. Biofouling on buoyant marine plastics: an experimental study into the effect of size on surface longevity. Environ. Pollut. 210, 354–360.
Guillard, R.R.L., 1975. In: Smith, W.L., Chanley, M.H. (Eds.), Culture of Phytoplankton for Feeding Marine Invertebrates, Culture of Marine Invertebrate Animals. Plenum Press, New York, pp. 26–60.
Hammer, Ø., Harper, D.A.T., Ryan, P.D., 2001. PAST: paleontological statistics software package for education and data analysis. Palaeontol. Electron. 4, 1–9.
Horton, A.A., Dixon, S.J., 2017. Microplastics: an introduction to environmental transport processes. WIREs Water 5, e1268.
Kiessling, T., Gutow, L., Thiel, M., 2015. Marine litter as habitat and dispersal vector. In: Bergmann, M., Gutow, L., Klages, M. (Eds.), Marine Anthropogenic Litter. Springer International Publishing, pp. 141–181.
Kontogiannopoulos, K.N., Dasargyri, A., Ottaviani, M.F., Cangiotti, M., Fessas, D., Papageorgiou, V.P., Assimopoulou, A.N., 2018. Advanced drug delivery nanosystems for Shikonin: a calorimetric and electron paramagnetic resonance study. Langmuir 34 (32), 9424–9434.
Long, M., Moriceau, B., Gallinari, M., Lambert, C., Huvet, A., Raffray, J., Soudant, P., 2015. Interactions between microplastics and phytoplankton aggregates: impact on their respective fates. Mar. Chem. 175, 39–46.
Mishraki, T., Ottaviani, M.F., Shames, A.I., Aserin, A., Garti, N., 2011. Structural effects of insulin-loading into HII mesophases monitored by EPR, SAXS, and ATR-FTIR. J. Phys. Chem. B 115 (25), 8054–8062.
Moriceau, B., Long, M., Paul-pont, I., Lambert, C., Huvet, A., Soudant, P., 2017. Interactions between polystyrene microplastics and marine phytoplankton lead to species-specific hetero-aggregation. Environ. Pollut. 228, 454–463.
Nguyen, H., Chen, Q., Paletta, J., Harvey, P., Jiang, Y., Zhang, H., Boska, M., Ottaviani, M.F., Jasanoff, A., Rajca, A., Johnson, J., 2017. Nitroxide-based macromolecular contrast agents with unprecedented transverse relaxivity and stability for magnetic resonance imaging of tumors. ACS Cent. Sci. 3 (7), 800–811.
Obbard, R.W., Sadri, S., Wong, Y.Q., Khitun, A.A., Baker, I., Thompson, R.C., 2014. Global warming releases microplastic legacy frozen in Arctic Sea ice. Earth's future 2, 315–320.
Oberbeckmann, S., Martin, A.C., Löder, M.G.J., Labrenz, M., 2015. Marine microplastic-associated biofilms - a review. Environ. Chem. 12, 551–562.
Ottaviani, M.F., El Brahmi, N., Cangiotti, M., Coppola, C., Buccella, F., Cresteil, T., Mignani, S., Caminade, A.M., Costes, J.P., Majoral, J.P., 2014. Comparative EPR studies of Cu(II)-conjugated phosphorous-dendrimers in the absence and presence of normal and cancer cells. RSC Adv. 4, 36573–36583.
Ottaviani, M.F., Pregnolato, M., Cangiotti, M., Fiorani, L., Fattori, A., Danani, A., 2012. Spin probe analysis of microtubules structure and formation. Arch. Biochem. Biophys. 522, 1–8.
Passow, U., 2002. Transparent exopolymer particles (TEP) in aquatic environments. Prog. Oceanogr. 55 (3–4), 287–333.
Reisser, J., Shaw, J., Hallegraeff, G., Proietti, M., Barnes, D.K., Thums, M., Wilcox, C., Hardesty, B.D., Pattiaratchi, C., 2014. Millimeter-sized marine plastics: a new pelagic habitat for microorganisms and invertebrates. PLoS One 9, e100289.
Van Sebille, E., England, M.H., Froyland, G., 2012. Origin, dynamics and evolution of ocean garbage patches from observed surface drifters. Environ. Res. Lett. 7, 044040.
Windsor, F.M., Durance, I., Horton, A.A., Thompson, R.C., Tyler, C.R., Ormerod, S.J., 2019. A catchment-scale perspective of plastic pollution. Glob. Chang. Biol. 25 (4), 1207–1221.
Zettler, E.R., Mincer, T.J., Amaral-Zettler, L.A., 2013. Life in the ‘plastisphere’: microbial communities on plastic marine debris. Environ. Sci. Technol. 47, 7137–7146.